Technical Paper:

Investigation of Internal Thread Cutting Phenomena in Three Axes by Controlling Helical Interpolate Motion Considering Tool Position Information from Servo-Drive

Shota Matsui*,†, Nobutoshi Ozaki*, Toshiki Hirogaki*, Eiichi Aoyama*, and Takamasa Yamamoto**

*Doshisha University
1-3 Tataramiyakodani, Kyotanabe-shi, Kyoto 610-0394, Japan
†Corresponding author, E-mail: adegu9@gmail.com
**Yamamoto Metal Technos Co., Ltd., Osaka, Japan
[Received September 17, 2019; accepted December 25, 2019]

In this study, the authors investigate improving the precision of a thread by deriving its radial force (thrust force) with a four-component piezoelectric dynamometer and thread cutting by helical interpolation motion using a thread mill. The accuracy of the thread is discussed with respect to changing hardness of the work material. In addition, by recording the position information at the time of thread cutting from the servo guide on the data logger, the relationships among the cutting forces of the four components and the radial force are confirmed by various methods; further, the consistency of these relationships was confirmed.

Keywords: thread-mill, machining center, internal thread cutting, cutting force, helical interpolation

1. Introduction

There has been considerable development in the field of motion of machine tools involving five-axis-controlled machining centers (5MC) and multi-functional turning centers to ensure high speed and high precision [1–3]. Further, the simultaneous motion accuracies of three axes at very high feed speeds have been greatly enhanced [4–6]. This possibility is owing to the development of control technology for machine tools. Additionally, the three-axis motion control accuracy for helical interpolation motion at high feed speeds applied at processing sites has reached a satisfactory level of advancement. Helical complementary motion has been employed as a processing method for boring [7–9] and pocket [10–12] processing of hard materials and appears to be a promising technology for use at processing sites. Presently, tool manufacturers are machining internal threads using thread mills, which create the screw threads using the cutting edges of the end-mill tool; this is garnering attention as a new processing technology that utilizes helical interpolation motion. In general, incorrect prediction of tool breakage is a problem in the tapping processing of difficult-to-cut materials, and research and development of methods to avoid this risk are essential [13–15]. In addition, by utilizing a method that combines the use of thread mills and helical interpolation motion, it is possible to use materials that are otherwise difficult to process via conventional tapping processing; these materials include ones with ultra-high hardness, such as composite materials, or super hard materials whose hardness changes remarkably during processing. Efficient cutting of such materials is therefore possible by this combination method, and it is expected that unpredictable failure of tools can be avoided in such instances. However, only a few systematic studies have attempted to describe internal thread cutting by thread mills using helical interpolation [16].

In this research, the influence of chatter vibration and machining accuracy of the work material on internal thread cutting was investigated for S50C [17]. We report our research on the processing accuracy of reading thread position information from the voltage output of the machine tool by confirming the thread accuracy of SKD61, which is a high-hardness steel material.

2. Proposed Internal Thread Method and Experimental Details

2.1. Internal Thread Using Thread Milling Tool

Figure 1 shows the relationship between a general external thread and an internal thread. Threads are essential fastening elements of machined element parts and are progressing toward standardization globally. Threads can roughly be categorized as metric threads or inch threads, according to the ISO standards, and are standardized mainly by the dimensions of the outer diameter and threads pitch. The threads considered in this work were coarse metric threads. The height of the thread cutting is the difference between the outer and inner diameters, as shown in **Fig. 1**. Often, the processing of these threads is easy because the external thread has threads that are cre-

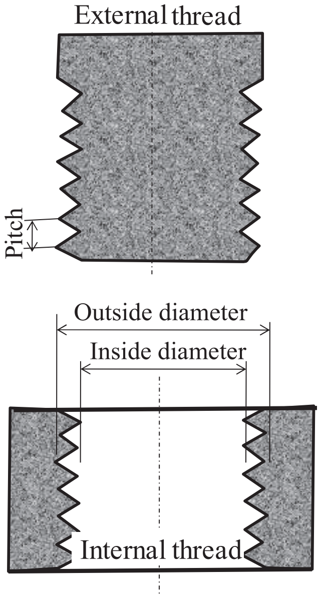

Fig. 1. Relationship between a general external thread and an internal thread.

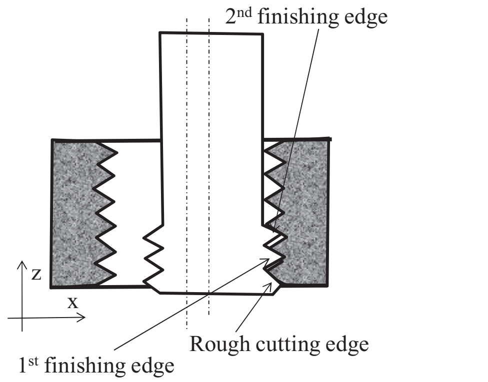

(a) Side cross section of thread milling tool during thread machining

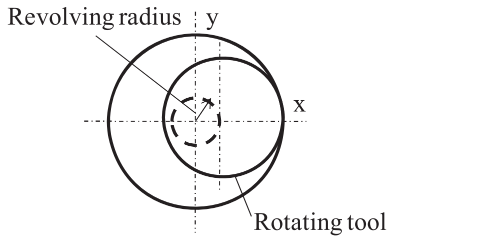

(b) Top view of thread processing

Fig. 2. Thread mill tool.

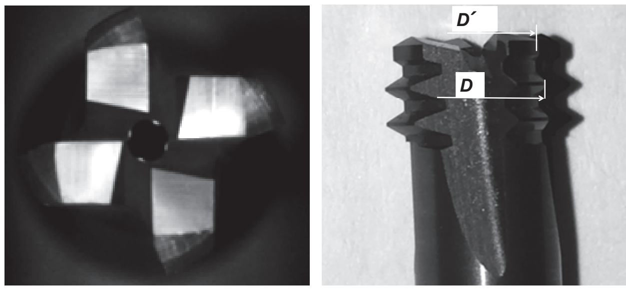

(a) End cutting edge (b) Side view

Fig. 3. Details of thread mill tool.

ated by outer diameter processing; however, processing of the internal thread often involves difficult techniques as it is necessary to create the thread crest by inner diameter processing. Machine parts, such as gears, require many internal thread elements, and often, stop internal threads are used in such cases. Therefore, this study focuses on the internal threads of blind holes. In most cases, a spiral tap is used for machining the internal thread of the blind hole [18–20]. However, it is difficult to increase the strength of the machined element part because the target material is difficult to grind and the breakage of the tap tool is a critical problem owing to clogging of chips during tapping. As a method to eliminate this problem, internal thread cutting using the thread mill tool is being developed, as shown in **Fig. 2**. The thread milling tool has a cutting edge with a screw thread whose height and pitch are matched with metric threads, and the outer diameter is smaller than the inner diameter of the thread to be machined. **Fig. 2(a)** shows a cross section view from the side surface during processing; the blade at the tip of the tool has a slightly smaller diameter of the cutting edge (diameter D' in **Fig. 3(b)**). The blade of the second pitch is thus used for the first finishing process, and the last (third) pitch is used as the tool shape (diameter D in **Fig. 3(b)**) for the final finishing ($D > D'$). In addition, by forming a cutting edge at the bottom of the tool, it is possible to perform thread processing even without pilot holes; **Fig. 2(b)** shows the top view of this condition. In the helical interpolation motion based on simultaneous three-axis numerical control in the xyz-directions, the tool first revolves in the clockwise direction and then in the counterclockwise direction while moving in the $-z$-direction by one pitch of the thread for one revolution. Unlike tapping, this method has no limitation on the number of rotations of the tool, and it is possible to appropriately select the number of rotations according to the characteristics of the workpiece. Because it is possible to secure a radial gap between the tool and the threaded hole, it is also possible to suppress chip clogging, which is a problem in the processing of difficult-to-cut materials. Meanwhile, as the gaps are secured in the radial direction, there are concerns regarding the influence of elastic deformation of the tool due to the cutting force, and studies are required to set the appropriate processing conditions by considering such deformations.

2.2. Apparatus and Cutting Force Measurement Method

The machine tool is MC (ACCUMILL 4000, DMG Mori Co., Ltd.). **Fig. 4** shows the schematic diagram of the cutting force measurement system. The tool is a thread mill (Epock D Thread Mill EDT-1.5-25-TH, Mitsubishi Hitachi Tool Engineering, Ltd.), as shown in **Fig. 5**, and the edge shape is shown in **Fig. 3**. From **Fig. 3**, it can be

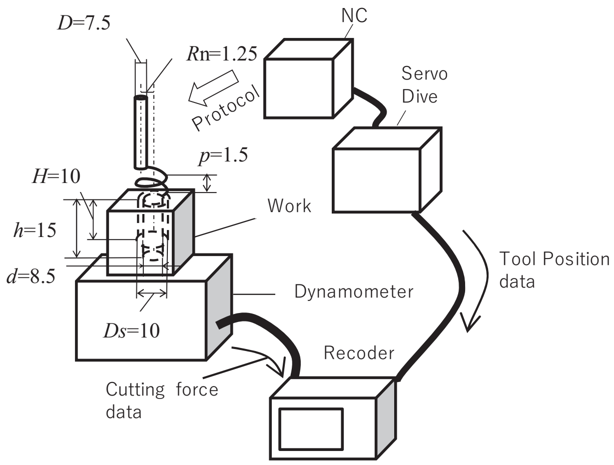

Fig. 4. Schematic of the internal thread cutting force monitoring.

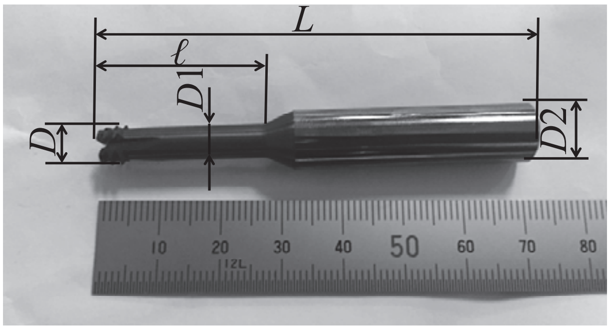

Fig. 5. Thread mill tool.

seen that the tool has a cutting edge on the bottom blade also, and the bottom cutting edge can perform internal thread cutting even without the under hole by the action of bottom cutting. The dimensions corresponding to **Figs. 3** and **5** are $D = \varphi 8.5$ mm, $D_1 = \varphi 5.5$ mm, $D_2 = \varphi 10$ mm, $L = 70$ mm, $\ell = 25$ mm, and $D' = \varphi 7.6$ mm, where D is the diameter of the finishing blade and D' is the diameter of the roughing blade. That is, $\ell/D_1 = 4.5$. The regular pilot hole diameter was processed at $\varphi 8.5$ mm. Further, S50C was used as the workpiece. The power of the four components was recorded by a data logger (midi LOGGER GL900 manufactured by GRAPHTEC Corporation) from a dynamometer (torque power diameter 9275 manufactured by KISTLER). To confirm the accuracy of the thread, a thread gauge (OSG-made grade 1 for work) was used. The cutting conditions are listed in **Table 1**. As a fundamental study, internal thread cutting was performed with $\varphi 8.5$ pilot diameters under a helical toolpath, using the NC helical interpolation command. The cutting conditions were set at a constant cutting speed of 35 m/min using the catalog conditions.

2.3. Derivation of Radial Force from *X*- and *Y*-Directions and the Torque Component

A method for deriving the principal cutting force (tangential force at the contact point of the workpiece of the tool) and thrust force (radial/normal direction at the contact point of the workpiece of the tool) from the measured X- and Y-directions forces and the torque component is presented in **Fig. 6**. A model diagram of measurement is shown in **Fig. 6**. The cutting force in the X-direction is F_x, that in the Y-direction is F_y, and the torque is T. The norm value of the resultant force in the X- and Y-directions is expressed by Eq. (1); the principal cutting force F_t is expressed by Eq. (2). The relationship between the resultant force value in the X- and Y-directions and the resultant force of the principal cutting force F_t and the thrust force F_n is shown in Eq. (3).

Table 1. Cutting condition.

Feed rate V_f	mm	57
Feed per tooth V_t	mm/tooth	0.038
Number of revolutions n	rpm	1500
Tool diameter D_1	mm	7.5
Coolant	–	Semi-dry
Rotational period of a tool T_1	s	0.04
Radius of the helical pass R_n	mm	1.25
Rotational period of the helical pass T_2	s	8.27
Core diameter D_s	mm	10
Pitch diameter of thread H	mm	10
Pitch p	mm	1.5
Hole before internal thread cutting diameter d	mm	8.5
Hole depth before internal thread cutting h	mm	15
Sampling time Δt	s	0.0002
Sampling frequency f_s	Hz	5000

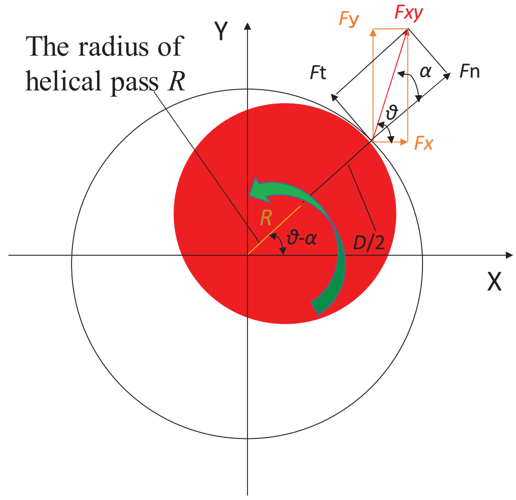

Fig. 6. Model diagram of measurement.

$$F_{xy} = \left(F_x^2 + F_y^2\right)^{\frac{1}{2}}, \quad \ldots \ldots \ldots \ldots (1)$$

$$F_t = \frac{T}{R_t}. \quad \ldots \ldots \ldots \ldots (2)$$

R_t is the total revolution center of the tool in helical interpolation and the radial distance from the center of rotation of the tool to the cutting point.

$$\left(F_x^2 + F_y^2\right)^{\frac{1}{2}} = \left(F_t^2 + F_n^2\right)^{\frac{1}{2}}. \quad \ldots \ldots \ldots (3)$$

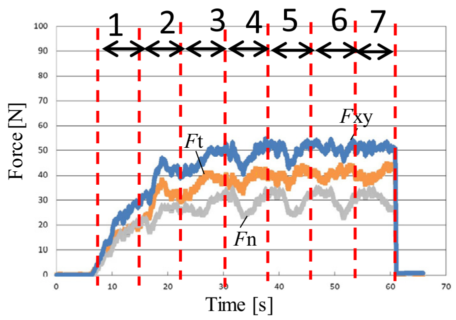

(a) S50C (150 Hv)

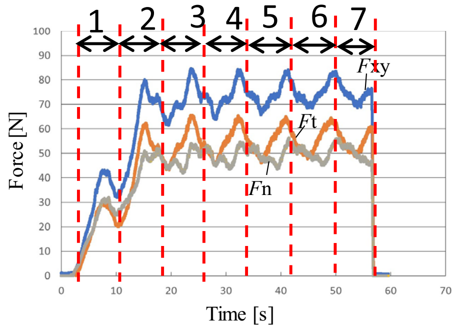

(b) SKD61 (400 Hv)

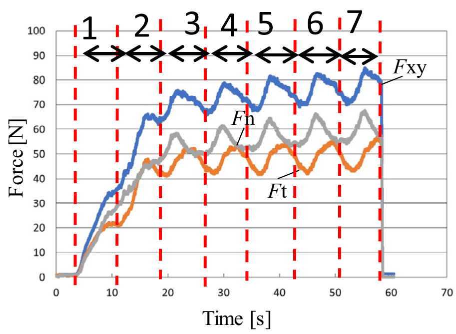

(c) SKD61 (600 Hv)

Fig. 7. Force vs. time.

From Eqs. (1)–(3),

$$F_n = \left(F_{xy}^2 - F_t^2\right)^{\frac{1}{2}} . \quad \quad (4)$$

In other words, using the outputs of X, Y and the torque components of a commercially available four-component dynamometer, it is possible to obtain the tangential force and radial force in machining by the rotary tool during the helical interpolation motion.

3. Experimental Results and Discussion

3.1. Workpiece Hardness and Cutting Force

The cutting force [N] for three types of work materials, S50C and SKD61 (HRC 40, 53), versus time [s] are shown in **Fig. 7**. **Fig. 7** shows the horizontal norm value F_{xy}, the tangential force (principal cutting force) F_t, and the radial force (thrust force) F_n. **Fig. 8** shows the cutting force [N] as a function of hardness [Hv] (6th cycle of

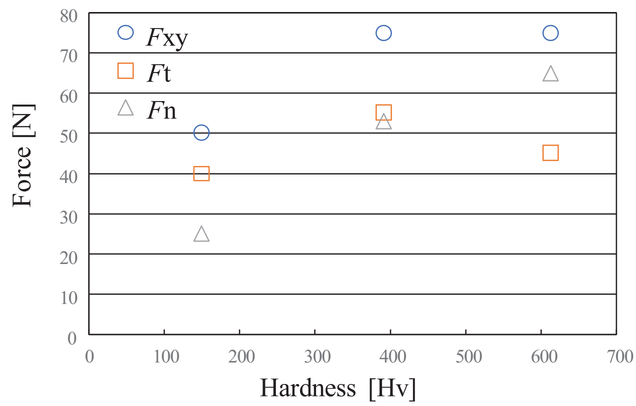

Fig. 8. Hardness vs. force.

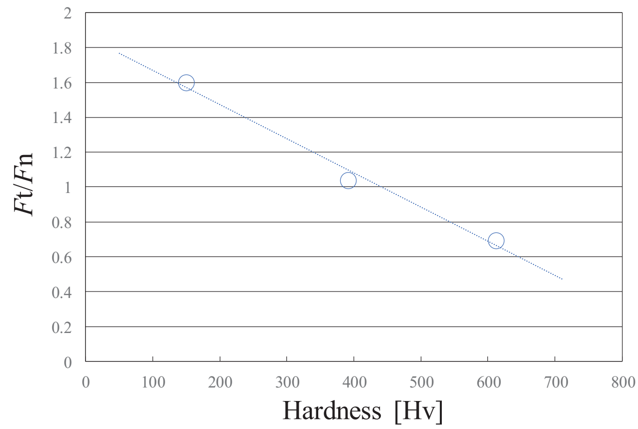

Fig. 9. Hardness vs. F_t/F_n.

revolution). **Fig. 9** shows the ratio of the main component to the back component versus the hardness [Hv]. As demonstrated in **Fig. 7**, F_{xy} rises to a certain hardness, but becomes constant above a certain hardness. Moreover, it was found that F_n increases as hardness increases, but F_t does not show the same tendency. In addition, **Fig. 9** shows that the ratio of F_t/F_n decreases as hardness increases. Since the tool has a negative rake angle, it can process even hard materials, and the difference in hardness becomes more pronounced in F_n (reverse force) than in F_t (main force) [17]. Therefore, F_n reacts especially when the material is hard, so the cutting accuracy (force in the X-, Y-, and Z-directions, torque T) output from the four-component dynamometer cannot guarantee the accuracy of the thread. For this reason, it is difficult to derive the radial force, and it is obvious that the radial force needs to be derived from the outputs of the four components.

3.2. Thread Accuracy and Revolution Radius Correction

Table 2 shows the results of accuracy measurement of the internal thread by using a thread gauge. After processing with S50C, SKD61 (HRC 40, 53) with a revolution radius R_n of 1.25 mm of a normal processing path,

Table 2. Result of gage test.

	Go	Not-go	Result
S50C $R_n = 1.250$	×	○	Small effective diameter
SKD61 (HRC40) $R_n = 1.250$	×	○	Small effective diameter
SKD61 (HRC53) $R_n = 1.250$	×	○	Small effective diameter
S50C zero cut	○	×	Large effective diameter
SKD61 (HRC40) zero cut	○	×	Large effective diameter
SKD61 (HRC53) zero cut	○	×	Large effective diameter
S50C $R_n = 1.270$	○	○	Good
SKD61 (HRC40) $R_n = 1.280$	○	○	Good
SKD61 (HRC53) $R_n = 1.285$	○	○	Good

when the accuracy is confirmed with a thread gauge, the passing side does not pass and the effective diameter of the internal thread is small. In addition, when a pass is performed in the same pass and in the case of a zero cut, the effective diameter through which the non-stop side of the thread gauge passes is large. Therefore, it is considered that, in the design of the tool used in this experiment, the amount of deflection in the tool radial direction is considered in advance. In order to ensure accuracy using this tool, it is necessary to correct and process the revolution radius of the machining path. In S50C and SKD61 (HRC 40, 53), the correction of the revolution radius of the processing path was possible within the accuracy of 0.020 mm, 0.030 mm, and 0.035 mm, respectively. The difference in radial force F_n between S50C and SKD61 is about 25 N and 35 N, and the tool used in this experiment has the holder end face fixed at one end and the other end free. Therefore, the deflection in the radial direction is obtained using Eq. (5).

$$v = \frac{64P\ell^3}{3\pi E D_1^4} \cdot \quad \cdots \cdots \cdots \quad (5)$$

where v is the radial deflection, E is the Young's modulus, and P is the force applied to the beam. Assuming a Young's modulus $E = 560$ GPa, the deflection amount in Eq. (5) is 0.009 mm and 0.013 mm, and the difference between the correction amount at each hardness of S50C and SKD61 in this experiment, is 0.010 mm and 0.015 mm. The values are almost the same, and it is clear that this correction is appropriate.

3.3. Change of Work Material and Vibration Analysis

In order to improve the accuracy of the thread and understand the vibration characteristics during machining, the cutting force in the X-direction is subjected to FFT analysis. The results of the FFT analysis of X-directional cutting force when S50C and SKD61 (HRC 53) are processed are shown in **Figs. 10** and **11**, respectively. When **Figs. 10** and **11** are compared, the peak points are shown

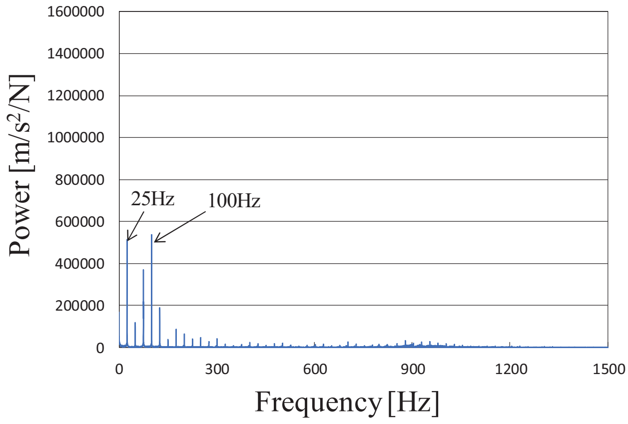

Fig. 10. Result of FFT (S50C).

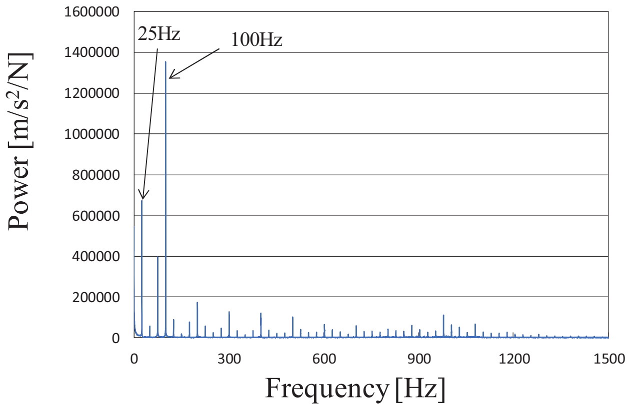

Fig. 11. Result of FFT (SKD61).

around 25 and 100 Hz; it can thus be seen that, although there is a difference in the work material, the same spectral tendency is seen in the vibration characteristics. The frequency of one tool rotation at a rotational speed of 1500 rpm is 25 Hz. The tool is a 4-flute tool, and the frequency per blade is 100 Hz. Therefore, the results of the vibration analysis of S50C, the power spectrum values, which are influenced by the tool shake and cutting edge, are similar for one rotation at frequencies of 25 and 100 Hz. For SKD61, the power spectrum value at 100 Hz is higher than that at 25 Hz. This result shows that when tool deflection due to F_n (radial force) is small, tool deflection has a relatively large effect. Conversely, when the deflection is large, each blade is equally involved in cutting. Further, in the norm value F_{xy} in **Fig. 8**, the ratio of S50C to SKD61 was approximately 1.3 times, but this ratio at 100 Hz, as shown in **Fig. 11**, is twice or greater than that shown in **Fig. 10**. It also shows that the power is increasing.

3.4. Output of Position Information from Servo Drive Unit

As shown in **Fig. 4**, the servo drive unit and dynamometer are connected to the same recorder, so the tool position and cutting force can be synchronized. This makes it

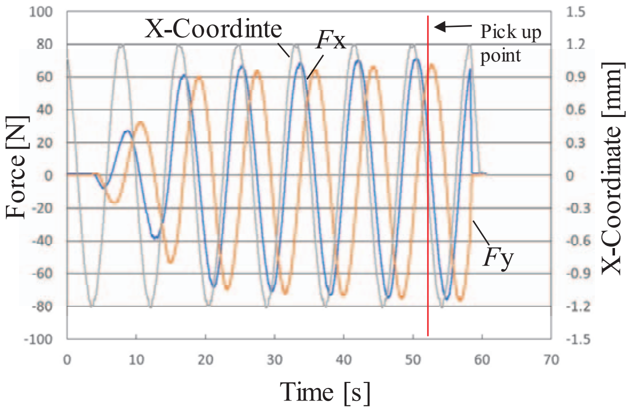

Fig. 12. Force, X-coordinate-time (SKD61).

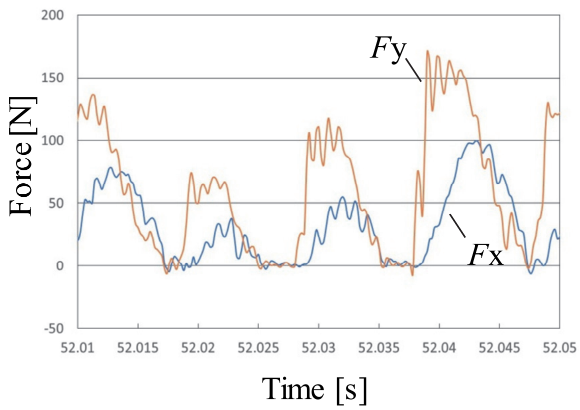

Fig. 13. One-rotation cycle of tool center (F_x, F_y).

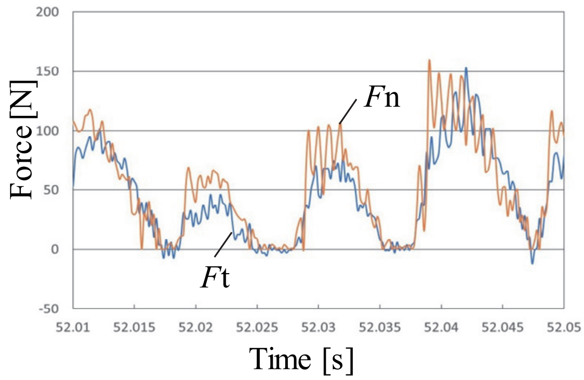

Fig. 14. One-rotation cycle of tool center (F_t, F_n).

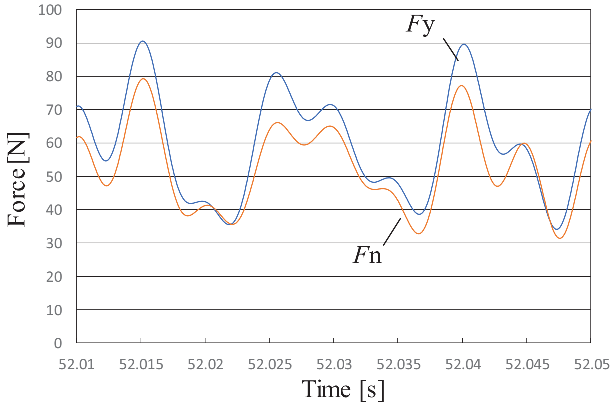

Fig. 15. Result of IFT (F_y, F_n).

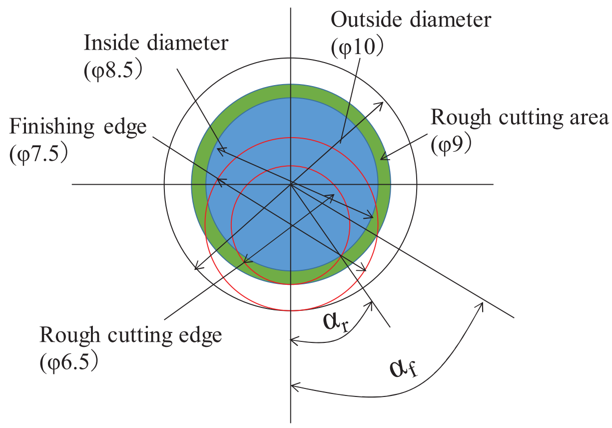

Fig. 16. Processing model.

possible to clarify the relationship between the tool position and cutting force. The relationship between the cutting force in the X- and Y-directions when processing SKD61 (HRC53) and the position information of the X-axis output from the servo guide is shown in **Fig. 12** (the coordinate relationship used **Fig. 6**). **Fig. 13** shows the raw waveform of the cutting forces F_x and F_y in the X- and Y-directions during one rotation of the tool when $\theta - \alpha = 270°$ when machining SKD61 (HRC53). **Fig. 14** shows the raw waveforms of the tangential force F_t and the radial force F_n during one rotation of the tool when $\theta - \alpha = 270°$. The extraction position in **Figs. 13** and **14** is the indicated position in **Fig. 8**. At the position of $\theta - \alpha = 270°$, $F_x \fallingdotseq F_t$ and $F_y \fallingdotseq F_n$. A comparison of **Figs. 13** and **14** shows that they are considerably different. **Fig. 15** shows the inverse Fourier transform of the cutting force F_y and the radial force F_n in the Y-direction, excluding the 100 Hz and 25 Hz cut cycles, when using a low pass filter at a frequency of 200 Hz or less. In **Fig. 15**, $F_n \fallingdotseq 0.8F_y$. A model of tool processing used in this experiment is shown in **Fig. 16**. Let α_r and α_f be the angles from the center of revolution of the contact point of the roughing blade and finishing blade, respectively. The difference between F_y and F_n can be expressed using Eq. (6).

$$F_n \fallingdotseq \cos\frac{\alpha_r + \alpha_f}{2}. \quad \ldots \ldots \ldots \quad (6)$$

In this experiment, Eq. (6) is about 35°. The radial force F_n is considered to be 80% of the cutting force F_y in the Y-direction and can be estimated to be approximately equal to the present derivation equation.

4. Conclusions

The forces and torques in the X-, Y-, and Z-directions during internal thread cutting with a thread mill were investigated using the helical interpolation function of a 3-axis control machining center. The relationship between the main component and thrust force was derived. The thread accuracy after machining was also examined for an M10 thread. The results are summarized below.

1) The ratio of radial force (thrust force) increases as the hardness of the work material increases.

2) The amount of correction in the radial direction can be derived, regardless of the hardness of the work material, by deriving the radial force with the proposed method.

3) It is possible to derive the radial force (thrust force) by acquiring tool position information using servo information, and it can be confirmed that it matches the radial force (thrust force) derived using the proposed method.

References:

[1] T. Ikegami, T. Hirogaki, and E. Aoyama, "Development of Automatic Servo Tuning Function in Rotary Axis with DDM for Machine Tools and its Performance for Stable Machining," J. Materials Sci. Forum, Vol.874, pp. 511-516, 2016.

[2] T. Suzuki, K. Yoshikawa, T. Hirogaki, E. Aoyama, and T. Ikegami, "Improved Method for Synchronizing Motion Accuracy of Linear and Rotary Axes Under Constant Feed Speed Vector at End Milling Point – Investigation of Motion Error Under NC-Commanded Motion –," Int. J. Automation Technol., Vol.13, No.5, pp. 679-690, 2019.

[3] K. Nakamoto and Y. Takeuchi, "Recent Advances in Multiaxis Control and Multitasking Machining," Int. J. Automation Technol., Vol.11, No.2, pp. 140-154, 2017.

[4] Z. Li, Q. Liu, X. Ming, X. Wang, and Y. Dong, "Cutting force prediction and analytical solution of regenerative chatter stability for helical milling operation," Int. J. Adv. Manuf. Technol., Vol.73, pp. 433-442, 2014.

[5] B. Sencer and Y. Altintas, "Identification of 5-Axis Machine Tools Feed Drive Systems for Contouring Simulation," Int. J. Automation Technol., Vol.5, No.3, pp. 377-386, 2011.

[6] M. Sudo, "Advanced Control Technologies for 5-Axis Machining," Int. J. Automation Technol., Vol.1, No.2, pp. 108-109, 2007.

[7] G. M. Zhang and S. G. Kapoor, "Dynamic Modeling and Analysis of Boring Machining System," J. Eng. Ind., Vol.109, pp. 219-226, 2001.

[8] B. Moetakef-Imani and N. Z. Yussefian, "Dynamic simulation of boring process," Int. J. Mach. Tools Manuf., Vol.49, No.14, pp. 1096-1103, 2009.

[9] C. Mei, "Active regenerative chatter suppression during boring manufacturing process," J. Robotics and Computer-Integrated Manuf., Vol.21, No.2, pp. 153-158, 2005.

[10] M. B. Bieterman and D. R. Sandstrom, "A Curvilinear Tool-Path Method for Pocket Machining," Proc. ASME 2002 Int. Mech. Eng. Congress Expos, pp. 149-158, 2002.

[11] H. S. Choy and K. W. Chan, "A corner-looping based tool path for pocket milling," Computer-Aided Design, Vol.35, No.2, pp. 155-166, 2003.

[12] C. Gologle and N. Sakarya, "The effects of cutter path strategies on surface roughness of pocket milling of 1.2738 steel based on Taguchi method," J. Materials Processing Technol., Vol.206, Nos.1-3, pp. 7-15, 2008.

[13] Y. Yamaoka, Y. Kakino, and T. Sato, "High Speed and High Productive Tapping by Intelligent Machine Tools (3rd Report) – Prevention of Tap Tool Breakage and Monitoring of Tool Failure for Difficult-to-machine Materials by Real-time Adaptive Control," J. JSPE, Vol.68, No.9, pp. 1226-228, 2002 (in Japanese).

[14] R. Matsuda, M. Shindou, T. Hirogaki, and E. Aoyama, "Monitoring of Rotational Vibration in Tap and Endmill Processes with a Wireless Multifunctional Tool Holder System," Int. J. Automation Technol., Vol.12, No.6, pp. 876-882, 2018.

[15] D. Zhang and D. Chen, "Relief-face friction in vibration tapping," Int. J. Mechanical Sciences, Vol.40, No.12, pp. 1209-1222, 1998.

[16] G. Fromentin and G. Poulachon, "Geometrical analysis of thread milling-part 1: evaluation of tool angles," Int. J. Adv. Manuf. Technol., Vol.49, pp. 73-80, 2010.

[17] S. Matsui, N. Ozaki, T. Hirogaki, E. Aoyama, and M. Shindo, "Study of screw cutting based on numerical controlled helical interpolation motion," J. of the Japan Society for Abrasive Technology, Vol.62, No.12, pp. 632-637, 2018 (in Japanese).

[18] T. Cao and J. W. Sutherland, "Investigation of thread tapping load characteristics through mechanistics modeling and experimentation," Int. J. Mach. Tools Manuf., Vol.42, No.14, pp. 1527-1538, 2002.

[19] S. C. Veldhuis, G. K. Dosbaeva, and G. Benga, "Application of ultra-thin fluorine-content lubricating films to reduce tool/workpiece adhesive interaction during thread-cutting operations," Int. J. Mach. Tools Manuf., Vol.47, Nos.3-4, pp. 521-528, 2007.

[20] O. A. Mezentsev, R. Zhu, R. E. Devor, S. G. Kapoor, and W. A. Kline, "Use of radial forces for fault detection in tapping," Int. J. Mach. Tools Manuf., Vol.42, No.4, pp. 497-488, 2002.

Name:
Shota Matsui

Affiliation:
Doctoral Student, Doshisha University

Address:
1-3 Tataramiyakodani, Kyotanabe-shi, Kyoto 610-0394, Japan

Brief Biographical History:
2013- Daiwa Gear Manufacturing Co., Ltd.
2018- Doctoral Student, Doshisha University

Main Works:
• "Investigation of Screw Cutting by Numerical Controlled Helical Interpolation Motion with a Machining Center," The Harris Science Review of Doshisha University, Vol.58, No.3, pp. 111-117, 2017 (in Japanese).
• "Study of screw cutting based on numerical controlled helical interpolation motion," J. of the Japan Society for Abrasive Technology, Vol.62, No.12, pp. 632-637, 2018 (in Japanese).
• "Consideration of machining phenomena based on tool rotation coordinate system monitor of threading of helical interpolation thread mill," J. of the Japan Society for Abrasive Technology, Vol.64, No.5, pp. 260-266, 2020 (in Japanese).

Membership in Academic Societies:
• Japan Society of Mechanical Engineers (JSME)
• Japan Society for Precision Engineering (JSPE)
• Japan Society for Abrasive Technology (JSAT)

Name:
Nobutoshi Ozaki

Affiliation:
Master Course Student, Doshisha University

Address:
1-3 Tataramiyakodani, Kyotanabe-shi, Kyoto 610-0394, Japan

Brief Biographical History:
2018- Master Course Student, Doshisha University

Main Works:
- "State estimation based on image processing of chatter mark on end-milled surface by two-dimensional discrete Fourier transform," Trans. of the Japan Society of Mechanical Engineers, Vol.85, No.879, 19-00292, 2019 (in Japanese).

Membership in Academic Societies:
- Japan Society of Mechanical Engineers (JSME)
- Japan Society for Precision Engineering (JSPE)

Name:
Toshiki Hirogaki

Affiliation:
Professor, Faculty of Science and Engineering, Doshisha University

Address:
1-3 Tataramiyakodani, Kyotanabe-shi, Kyoto 610-0394, Japan

Brief Biographical History:
1990- Mitsubishi Motors Corporation
1993- Technology Research Institute of Osaka Prefecture
1995- The University of Shiga Prefecture
2003- Doshisha University
2006-2007 Visiting Researcher, University of California, Berkeley

Main Works:
- "Environmental Impact of Desktop-Sized Five-Axis CNC Machine Tool Estimated with LCA," J. of Environment and Engineering, Vol.6, No.2, pp. 242-252, 2011.
- "Control of Percussion Motion by Sound Feedback with a Humanoid Robot," Int. J. of Key Engineering Materials (Emerging Technology in Precision Engineering XIV), Vols.523-524, pp. 699-704, 2012.
- "Investigation of Temperature Hysteresis on Tooth Contact Surface of Hypoid Gears using Middle-infrared ray Imagery Based on Thermal Network model," J. of Advanced Mechanical Design, Systems, and Manufacturing, Vol.8, No.3, 13-00319, 2014.
- "Improving Method of Synchronizing Motion Accuracy of Rotary Axes and Linear Axis under Constant Feed Speed Vector at End Milling Point – Investigation of Motion Error Under NC-Commanded Motion –," Int. J. Automation Technol., Vol.13, No.5, pp. 679-690, 2019.

Membership in Academic Societies:
- Japan Society of Mechanical Engineers (JSME)
- Japan Society for Precision Engineering (JSPE)
- Society of Materials Science, Japan (JSMS)
- Japan Institute of Electronic Packaging (JIEP)

Name:
Eiichi Aoyama

Affiliation:
Professor, Faculty of Science and Engineering, Doshisha University

Address:
1-3 Tataramiyakodani, Kyotanabe-shi, Kyoto 610-0394, Japan

Brief Biographical History:
1977- Technology Research Institute of Osaka Prefecture
1987- Doshisha University
1997-1998 Visiting Researcher, Queen Mary & Westfield College, University of London

Main Works:
- "Estimation of Micro-hole Shape in Laser Direct Drilling of High Heat Radiation Typed Printed Circuit Boards (Process Monitoring with a High Speed Camera)," J. of Key Engineering Materials, Vol.625 (Precision Engineering and Nanotechnology V), pp. 172-177, 2014.
- "An Indicative End-milling Condition Decision Support System Using Data-Mining for Difficult-to-cut Materials Based on Comparison with Irregular Pitch and Lead End-mill and General Purpose End-mill," J. of Advanced Materials Research, Vol.797, pp. 177-182, 2013.
- "Surface Generation for Magic-Mirror by End-Milling and Magnetic Polishing with Digitally Functioned CNC Machining Center," J. of Key Engineering Materials (Emerging Technology in Precision Engineering XIV), Vols.523-524, pp. 368-373, 2012.

Membership in Academic Societies:
- Japan Society of Mechanical Engineers (JSME)
- Japan Society for Precision Engineering (JSPE)
- Japan Society for Abrasive Technology (JSAT)
- Society of Materials Science, Japan (JSMS)

Name:
Takamasa Yamamoto

Affiliation:
Senior Research Engineer, Yamamoto Metal Technos Co., Ltd.

Address:
2-4-7 Setoguchi, Hirano-ku, Osaka 547-0034, Japan

Brief Biographical History:
2013- Yamamoto Metal Technos Co., Ltd.

Main Works:
- "Development of Wireless Communication Tool Holder for Smart Factory in Next Generation and Its Application of Self-Monitoring of Spindle Equipped with Machine Tools," The Harris Science Review of Doshisha University, Vol.60, No.2, pp. 87-93, 2019 (in Japanese).
- "Investigation of spindle state diagnosis and processing phenomenon monitor with a wireless multifunctional tool holder system," J. of the Japan Society for Abrasive Technology, Vol.64, No.2, pp. 91-97, 2020 (in Japanese).

Membership in Academic Societies:
- Japan Society of Mechanical Engineers (JSME)
- Japan Society for Abrasive Technology (JSAT)